ISSN 2176-5480

22nd International Congress of Mechanical Engineering (COBEM 2013)
November 3-7, 2013, Ribeirão Preto, SP, Brazil

FLOW OF OIL DROPS THROUGH MICRO CAPILLARIES

José Angel Florián Gutiérrez
Marcio S. Carvalho
Department of Mechanical Engineering
Pontificia Universidade Católica do Rio de Janeiro (PUC)
Rua Mârques de São Vicente, 225, Gávea-Rio de Janeiro, RJ-Brasil
CEP 22451-900
joseangel@aluno.puc-rio.br
msc@puc-rio.br

Abstract. *This work presents an analysis of the flow of oil drops suspended in water through microchannels with constant cross-section area and with a throat, that are used as models for the pore space of a porous media. The velocity field of the continuous phase and the drop velocity are obtained using the micro particle image velocimetry (μ-PIV) for different drop sizes and microchannel geometries. The results show the changes in the flow pattern due to the presence of oil drops and yields important information on how oil drops reduce the mobility of the injected liquid when it flows through pore throats smaller than the drop size.*

Keywords: *Oil Drop, Emulsion, Capillarity, Micro PIV, Micro capillary*

1. INTRODUCTION

The enhanced oil recovery method most used is water injection, however, the water front into the reservoir is non-uniform due to an unfavorable mobility ratio between the oil and water phases caused by the difference of viscosity between them, with the appearance of interface configurations called fingers.

Oil-water emulsions can be used as an alternative with the ability to block the pores already swept by water injection. “Figure 1” shows a schematic illustration of the process of blocking pores by oil drops and redistribution the flow of the aqueous phase. “Figure 1” also shows the representation of the pore space as straight and constricted capillaries.

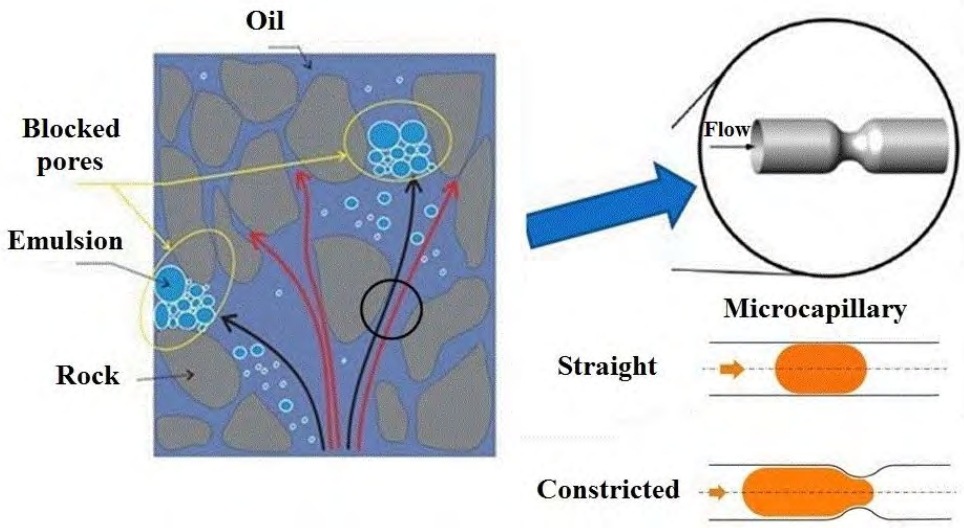

Figure 1. Schematic representation of the locking mechanism by emulsions injection

In recent studies “Guillen, *et al*., 2012” show that injection of oil-in-water emulsions acts at the macroscopic and pore scales leading to an increase of oil recovery factor. To optimize this process, it is essential to have a perfect understanding how emulsions flow through porous media, particularly through the pore throats.

Several studies in the literature show flow of a fluid suspended in another fluid through capillaries with constant cross section (Ho and Leal, 1975). Few studies have been done in capillaries with throat and most of these were focused on the relation between flow and differential pressure as function of flow conditions (Olbricht and Leal, 1983). Details of the velocity field around the drops were described only by numerical solutions (Martinez and Udell, 1990).

ISSN 2176-5480

This work was focused on the flow of oil drops suspended in an aqueous phase through microchannels with constant cross-section area and with a throat, to determine the effects of capillary geometry, throat and drop size in the velocity field of an emulsion's flow using the technique of particle image velocimetry in a micrometer scale.

2. APPARATUS AND EXPERIMENTAL TECHNIQUE

2.1 Experimental set-up

The experimental set-up is shown schematically in "Fig. 2"; it is composed by two main systems:

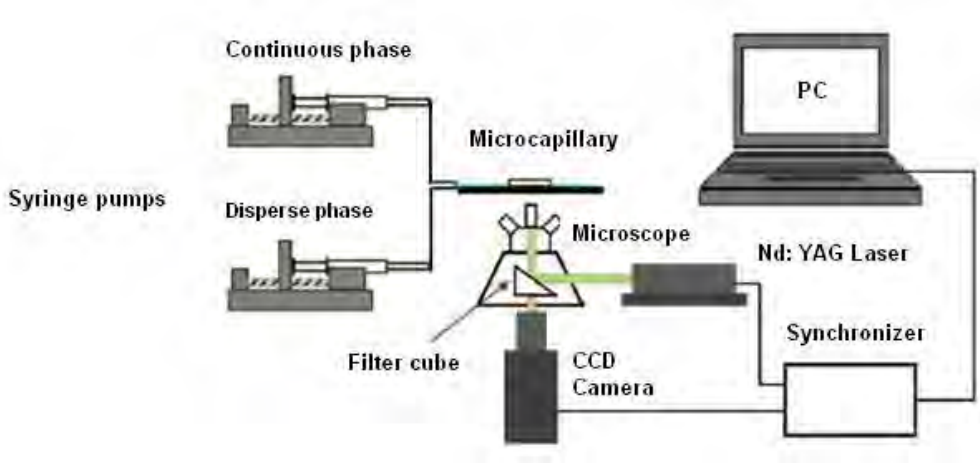

Figure 2. Scheme of the experimental setup of the measurement of the velocity field

The injection system consists of a micro capillary, two syringe pumps, two syringes and accessories used for mounting the flow circuit, as shows in "Fig. 3". The glass microcapillary used has straight microchannels with oval cross section, and a throat of length, maximum and minimum diameter of 70 µm, 110 µm and 85, µm respectively, as shown in "Fig. 4", manufactured by Dolomite Centre Ltd, UK. The syringe pumps Cole-Parmer®, models 78-0100C and 78-0200C, were used in the injection of the continuous and dispersed phase. The continuous phase fluid was composed of a mixture of distilled water with Sodium Dodecyl Sulfate $C_{12}H_{25}NaO_4S$ (6.9 g/l, three times its critical micelle concentration) surfactant and seeded with Fluoro-Max™ polymer microspheres supplied by Thermo Scientific with diameters equal to 1 µm. The disperse phase fluid was Drakeol 7 mineral oil. The Hamilton Gastight glass syringes were used for each phase with volume of 1ml.

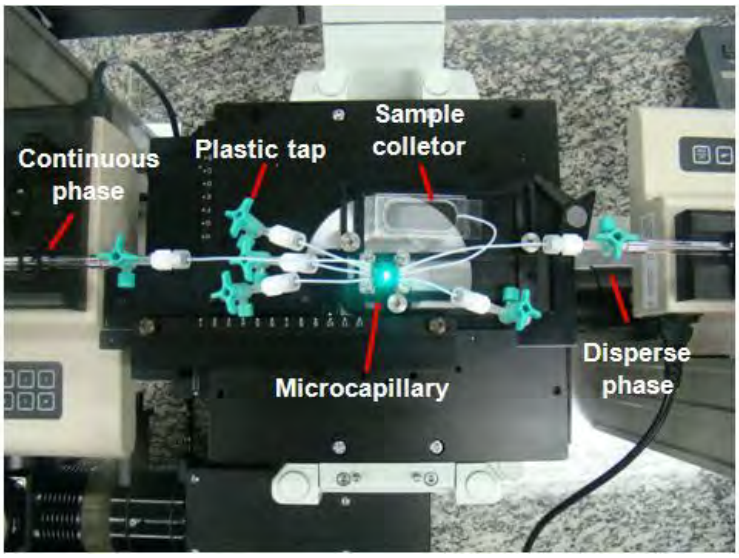

Figure 3. Mounting the injection system of the continuous and dispersed phase in the µ-PIV system

ISSN 2176-5480

Figure 4. Cross section of the channels and dimensions of the throat

The µ-PIV (Micro-Particle Image Velocimetry) system is composed by an Olympus® Inverted microscope; model IX71S1F-3, with an Olympus® UPlanFLN 10x/0.30 objective. A PowerView CCD 1.4MP Sensicam Mod-630066 camera was used to capture images of the illuminated tracer particles, with a resolution equals 1376x1040 pixels and a pixel size 6.45 µm x 6.45 µm. Two Nd:YAG (Neodymium: Yttrium-Aluminium-Gallium) model Gemini PIV-15 lasers were used to illuminate the flow through the microcapillary, with a wavelength of 532 nm, 50 mJ per energy pulse and a maximum frequency of 15 Hz, manufactured by NEW WAVE. The Laser Pulse Model 610034 synchronizer was used to control the timing sequence of shots of the laser pulse and exposure of the camera. The µ-PIV system was controlled by a computer using the Insight 3G™ software developed by the TSI® (Trust. Science. Innovation).

2.2 Experimental procedure

The experimental procedure was performed to measure the velocity field of single and two phase flow. "Figure 5" shows the microcapillary used for these measurements.

Figure 5. Microcapillary used, showing the input and output flow, the region of oil drop formation and the regions evaluated in the flow

In single phase flow, the injection flow of the continuous phase (distilled water seeded with fluorescent particles) was of 0.03 ml/h. The fluid enters the microcapillary by the aperture No. 1 and exits by the No. 2, and the apertures No. 3, 4, 5, 6 and 7 are closed by plastic taps. The region B was used to measure the velocity field in a straight microchannel with constant cross section, and the region C the flow near the throat.

In two phase flow, the injection flow of the continuous phase (mixture distilled water with surfactant and seeded with fluorescent particles) was of 0.03 ml/h and the disperse phase (oil) was of 0.003 ml/h. The continuous phase fluid enters the micro capillary by the aperture No. 1 and the disperse phase fluid enters by the aperture No. 4 and the output flow exits by the aperture No. 2, and the apertures No. 3, 5, 6 and 7 were closed by plastic taps. Region A (T junction) was used in the formation of oil drops, region B was used to measure the velocity field of flow near the drop in a straight microchannel with constant cross section, and the region C the flow near the drop in the throat.

For both flows, it was necessary to expel the air in the syringes, in the plastic taps and in the microcapillary, to avoid the presence of air bubbles that might have compromised the measurement of the velocity field. The calibration was of 0.41 µm /pixel and the particles concentration was of 0.14% suspended in distilled water. The laboratory temperature was set at 23°C.

The drop size was characterized by the drop radius R_g in its spherical configuration. R_g is calculated using the drop volume produced V_g, as shown in "Eq. (1)". The parameter α characterizes the relative size of the drop and the capillary, where R_c is the radius of the microcapillary, as shown in "Eq. (2)". For our case, α=1.4 (small drop).

ISSN 2176-5480

$$R_g = \left(\frac{3V_g}{4\pi} \right)^{1/3} \quad (1)$$

$$\alpha = \left(\frac{R_g}{R_C} \right) \quad (2)$$

2.3 Micro-PIV

The μ-PIV technique is an extension of the PIV method. The main difference between these two techniques is that the dimensions of flow in the μ-PIV system are much smaller, incorporating new optical techniques. According "Wereley, *et al*., 1998" there are three factors that differentiate the PIV from μ-PIV system. First, the tracer particles are small in comparison with the wavelength of light, requiring the use of fluorescence image in micro-PIV. Second, due to the smaller particle size, the Brownian motion can become a significant source of random error in the measurement of the displacement of the particles between images. Third, in the PIV system the flow is illuminated through a plane generated by the laser light, in micro-PIV the entire volume of the flow is illuminated.

The μ-PIV system consisted of a pulsed light source (laser), which was synchronized with the CCD camera that recorded two successive images (Frame LA and Frame LB) in a time interval. This technique is known as frame straddling.

The tracer particles used had a diameter of 1 μm and density of 1.05 g/cm^3, to minimize the effect of gravitational (floating and sedimentation) forces. The fluorescent lighting was used, the camera produced images of dark field and the particles appeared bright in the background.

Once the images of the tracer particles corresponding to the two light pulses have been recorded, the next step is to start the analysis of these images, with the goal of extracting information about the displacements of the particles and the desired velocity field.

The pre-processing step is used to improve the appearance of the captured images and to increase the signal to noise ratio, detecting and removing stationary particles, walls, scratches and smudges produced by the reflection of particles located outside the focal plane contributing to the background noise. There are several pre-processing techniques available. In the present work a minimum intensity image was generated from a sequence of raw images. This background intensity was removed from each original image using the technique of background subtraction to increase the signal to noise ratio and to obtain a better quality of the original images.

The processing step is used to extract information about the displacement of the particles and the desired velocity field. The cross correlation method was used and employed to determine the velocity field using two successive images of the flow. A pair of images may contain hundreds or thousands of particles, due to this; the images are divided into sub-areas called interrogation areas or spots, and by statistical methods are correlated to obtain the vector filed. However, the selection of the interrogation area should be adequate to get a good measurement of the velocity field. The number of particles for each interrogation area should be around 5-12 particles (Raffel, *et al*., 2002) and the displacement of the fluorescent particles should not exceed 25% of the size of the interrogation area (Prasad, 2000). To minimize the problems of an insufficient number of particles inside each interrogation area, to reduce the percentage error due to Brownian motion of the particles and to increase the signal to noise ratio in the correlation peak, the average correlation algorithm, also called Ensemble Average was used. The vector map is calculated based on the average correlation of multiple pairs of images. In single phase steady state flow, this technique consists of creating a vector field from the sample mean of several instantaneous fields. In two phase flow, the flow with drops in suspension, this technique becomes more complicated, because the flow is inherently transient. This problem was transposed in this case using the fact that the flow is periodic and that all drops are of the same size. The ensemble average was performed with images obtained with different drops located exactly in the same position of the channel. The processing was done through a single processing step "Nyquist Grid" and the starting and final spot dimensions were equal. For the correlation mapping was used the classical method of fast Fourier Transform "FFT Correlator", and in the location of the peak was used the Gaussian function "Gaussian Peak".

The post-processing step was done in the sequence of images to remove the false vectors, to fill holes and to smooth the vector field. First, the technique Vector Local Median was used to calculate a reference vector for validation, which uses the median of all the vectors in the neighborhood of each vector. Finally, the technique Vector Conditioning, which uses the average of the vectors of neighborhood around the hole to fill them, and low pass Gaussian filter to smooth the vector field. Both techniques were available in the Insight 3G^{TM} software.

3. RESULTS

ISSN 2176-5480

This section shows the results of the velocity fields of a single phase (water) and two phases (oil drops suspended in water) flow through a straight microchannel of constant cross section and a microchannel with a throat. “Figure 6” shows a scheme of the experiments performed in the single phase and two phase flow.

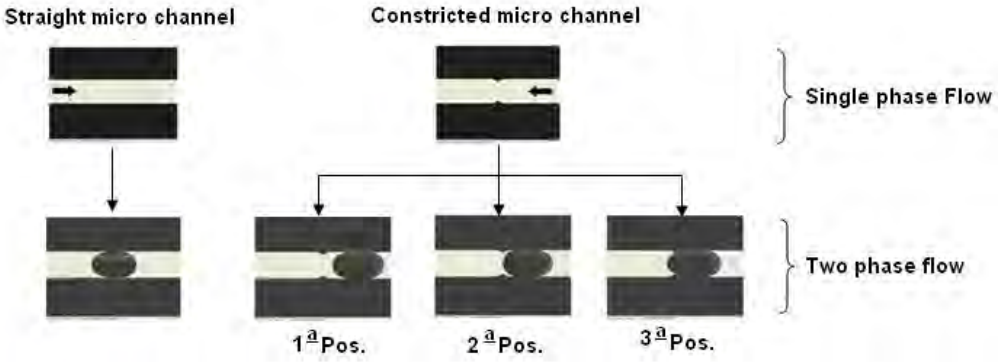

Figure 6. Scheme of the experiments performed

3.1 Measurement of the velocity field of single phase flow

The velocity fields were obtained from capturing images, the pre-processing, processing and post-processing techniques and masks used to process the desired flow area. The result obtained with the μ-PIV system in the case of the straight microchannel with constant cross section was compared with analytical solution of fully developed laminar flow and served as base case for comparison with the flow of drops suspended and to quantify the accuracy of measurements of the velocity field. In the case of the microchannel with throat the vector field was evaluated comparing the experimental average velocities at the input and output of the flow with the injection velocity imposed.

A selected area was defined by a mask for processing images; the dimensions were of 1376x269 pixels (approximately 564 μm length x 110 μm height) in the straight microchannel. In the microchannel with throat, the mask was adjusted to the geometry of the throat.

The capture timing setup was as follows: Pulse repetition rate for the laser was 4.83 Hz, the laser pulse delay was 800 μs, the exposure time of the camera was 1300 μs, and the pulse separation between the pair of images was of 1400 μs and 1200 μs for the straight and with throat microchannel, respectively. The spatial resolution was 32x32 pixels (13x13 μm^2).

“Figure 7” shows the velocity field of the flow in the straight microchannel, showing only 50% of the velocity profiles to facilitate the visualization of the vector field, and “Figure 8” shows the velocity field of the flow in the microchannel with throat. The velocity fields were obtained from 100 pairs of consecutive images processed using the Tecplot® software.

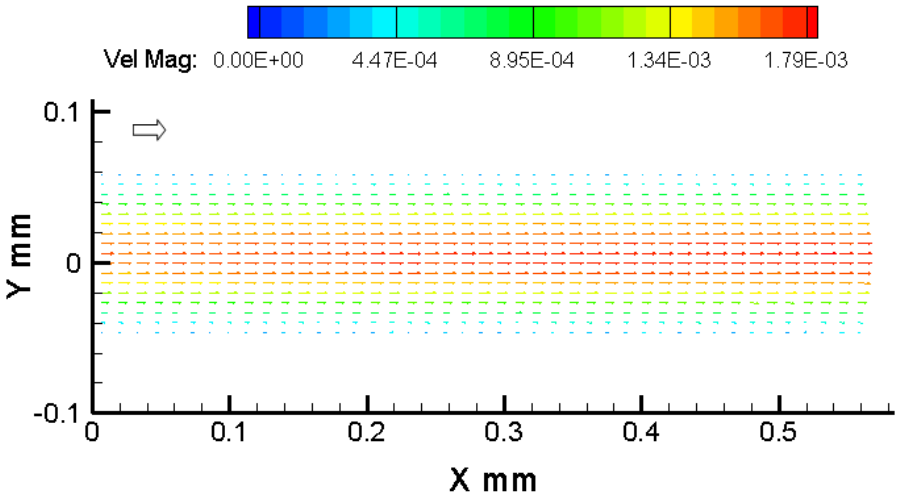

Figure 7. Velocity field of the flow through the straight microchannel

ISSN 2176-5480

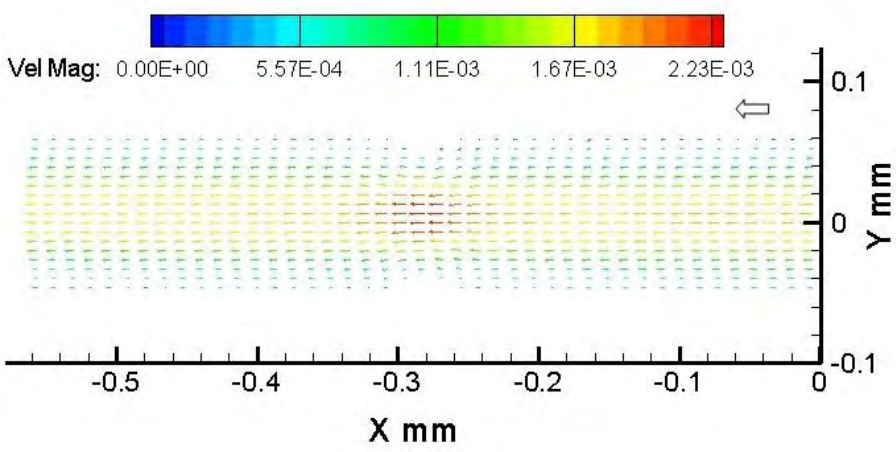

Figure 8. Velocity field of the flow through the microchannel with throat

In the straight microchannel, the flow shows the expected parabolic velocity profile. The experimental average velocity obtained from integration of the velocity profile was 8.73×10^{-4} m/s, while the actual injection average velocity was 8.77×10^{-4} m/s. The error percentage of the average velocity was only 0.44%. The experimental and analytical velocity profiles are show in "Fig 9", confirming the parabolic shape of experimental velocity profile, and that the measured values match the parabolic velocity profile.

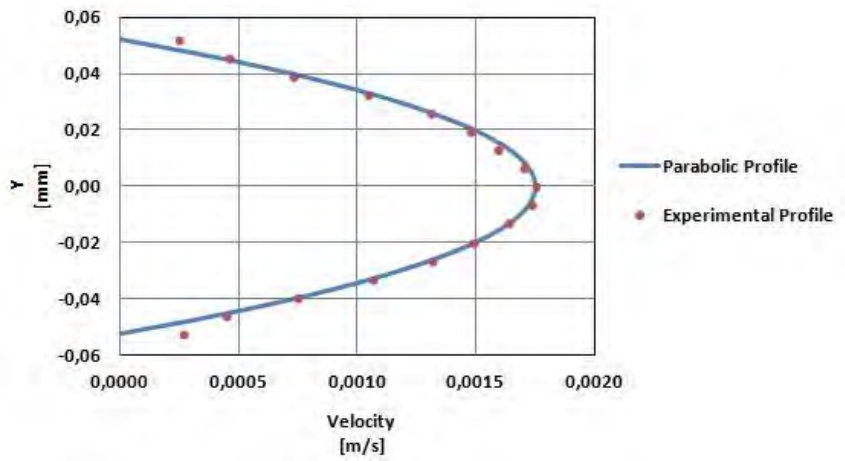

Figure 9. Comparison of experimental and parabolic profile through the straight microchannel

In the microchannel with throat, the experimental values of average velocity at the inflow and outflow phases are shown in "Tab. 1" together with the average injection velocity. It is observed that the maximum percentage error in the velocity was around 4%. “Figure 10” shows the experimental velocity profiles at the input and output of the flow and the theoretical velocity profile, note that the measured profile is very similar to the theoretical velocity distribution.

Table 1. Velocity values of the profiles of input and output of the flow through the microchannel with throat

	$V_{average}$ Injection ($x10^{-4}$ m/s)	$V_{average}$ Experimental ($x10^{-4}$ m/s)	Error %
Input profile	8.768	9.070	3.43
Output profile	8.768	8.640	1.47

ISSN 2176-5480

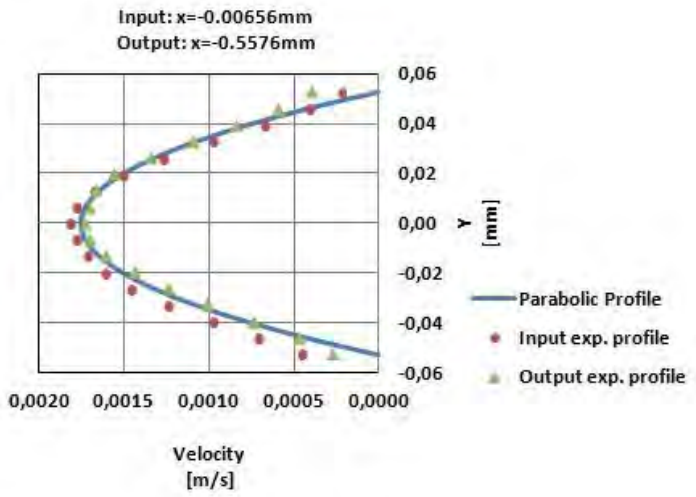

Figure 10. Comparison of parabolic profile and the experimental velocity profiles in the input and output of the flow through the microchannel with throat

3.2 Measurement of the velocity field of two phase flow

In the two phase flow the fluorescent particles were dispersed only in the aqueous phase, so that the drop appears as a dark smudge on the velocity field. The velocity field of the continuous phase (water) was determined for a fixed drop size and a capillary geometry. The drop velocity was determined by measuring the velocity of the continuous phase near the interface between the phases. For both cases (straight and with throat capillary), the velocity fields were obtained from capturing images, the pre-processing, processing and post-processing techniques and masks used to process the desired flow area.

In the case of straight microchannel, the area was defined by a mask, the dimensions were of 1376x269 pixels (approximately 564 µm length x 110 µm height) and the length of the drop was 213 µm (approximately 520 pixels). The capture timing setup was as follows: Pulse repetition rate for the laser was 4.83 Hz, the laser pulse delay was 800 µs, the exposure time of the camera was 1300 µs, and the pulse separation between the pair of images was 1000 µs. The spatial resolution was 32x32 pixels (13x13 μm^2).

"Figure 11" shows the velocity field of the flow around the oil drop, also showing 50% of the velocity profiles to facilitate the visualization of the vector field. The velocity field was obtained from 100 pairs of consecutive images processed using Tecplot® software.

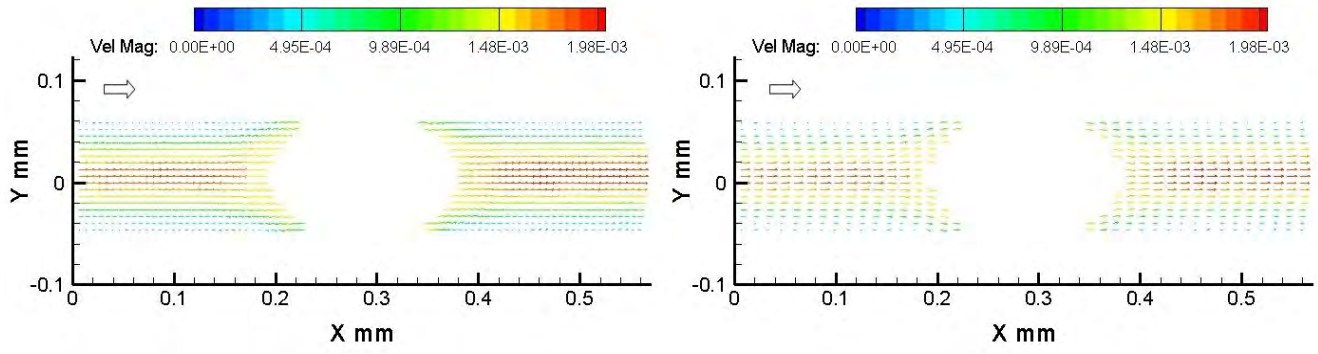

Figure 11. Velocity field of the flow around the drop through the straight microchannel

The experimental velocity profiles in the input and output of the flow are shown in "Fig 12" together with the theoretical velocity profile.

Far of the oil drop the flow of the continuous phase retrieves the developed parabolic profile. To determine the accuracy these measures, the measurements far of the drop were compared with the solution developed profile, as shows in "Tab. 2". The maximum percentage error in the velocity was approximately 5%.

The drop moves without deformation, so the velocity field around it is constant. Then the drop velocity was calculated through the average velocity in the oil-water interface upstream of the drop. The drop moves at a velocity

ISSN 2176-5480

greater than the mean flow approximately 1.5 times greater. The capillary number was Ca=1.6x10^{-4}. It is important to note that the measured value of V_g/V_m (V_g is the drop velocity and V_m is the average flow velocity) was higher than the value presented in the literature by (Lac and Sherwood, 2009). However, the range of parameters in previous studies was always for largest diameters capillaries and greater capillary number (Ca~>0.05).

Table 2. Velocity values of flow and the drop through the straight microchannel

Drop α=1.4	$V_{average}$ (V_m) Injection flow (x10^{-4} m/s)	$V_{average}$ Exp. Input profile (x10^{-4} m/s)	$V_{average}$ Exp. Output profile (x10^{-4} m/s)	V_g Drop Veloc. (x10^{-4} m/s)	V_g/V_m
100 Images	9.499	9.080	9.270	14.85	1.56

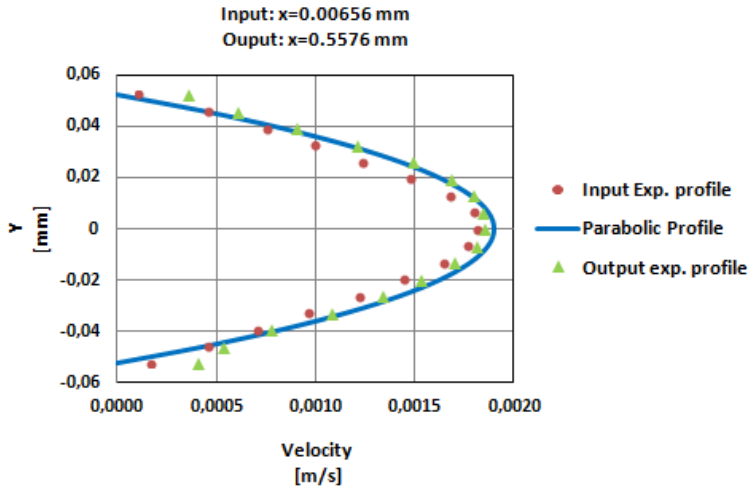

Figure 12. Comparison of parabolic profile and the experimental velocity profiles in the input and output of the flow around the drop, through the straight microchannel

Details of the flow can be studied analyzing the flow of the continuous phase relative to the drop. To obtain the velocity field relative to the drop, the drop velocity was subtracted from the velocity field of the two phase flow. "Figure 13" shows the velocity field relative to the drop, also showing 50% of the speed profiles to facilitate the visualization. In the velocity field there are two flows traveling in different directions. The suspension flow in the central part of microcapillary moves a greater velocity than the drop (in the same direction of the drop), and the suspension fluid adjacent to the well of the microcapillary move a lower velocity than the drop (in the opposite direction of the drop). "Figure 14" shows the streamlines of the flow of the continuous phase in the velocity field relative to the drop.

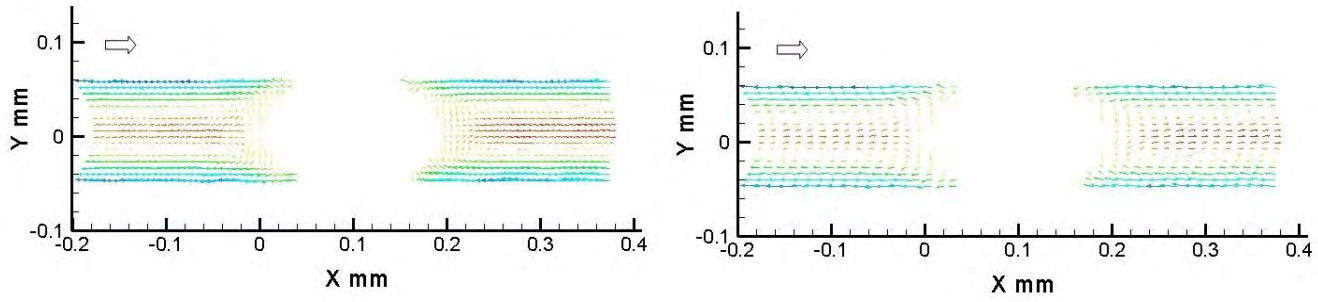

Figure 13. Velocity field relative to the drop through the straight microchannel

ISSN 2176-5480

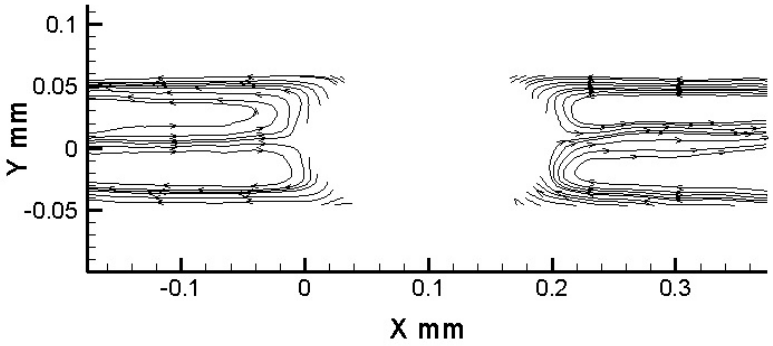

Figure 14. Streamlines of the flow around the drop through the straight microchannel

In the case of the microchannel with throat, to study the evolution of the flow during the passage of the drop by the throat, the velocity field was determined for three different positions of the drop along the throat. In the first position, the tip of the drop is located at the beginning of the throat, in the second position on the plane of lower cross section and third position the tip of the drop is located the end of the throat, as shows in "Fig 15".

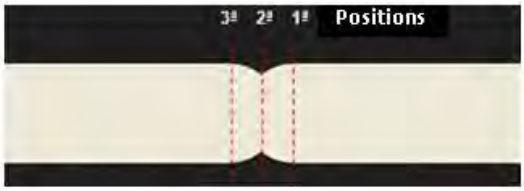

Figure 15. Streamlines of the flow around the drop through the straight microchannel

The area selected for processing images was defined through a mask for each position of the drop. The capture timing setup was as follows: Pulse repetition rate for the laser was 4.83 Hz, the laser pulse delay was 800 µs, the exposure time of the camera was 1300 µs, and the pulse separation between the pair of images was 1000 µs. The spatial resolution was 32x32 pixels (13x13 μm^2).

"Figures 16, 17 and 18" show the velocity fields of the flow around the oil drop for each position, also showing 50% of the velocity profiles to facilitate the visualization of the vector field. The velocity fields were obtained from 50 pairs of consecutive images processed using the Tecplot® software.

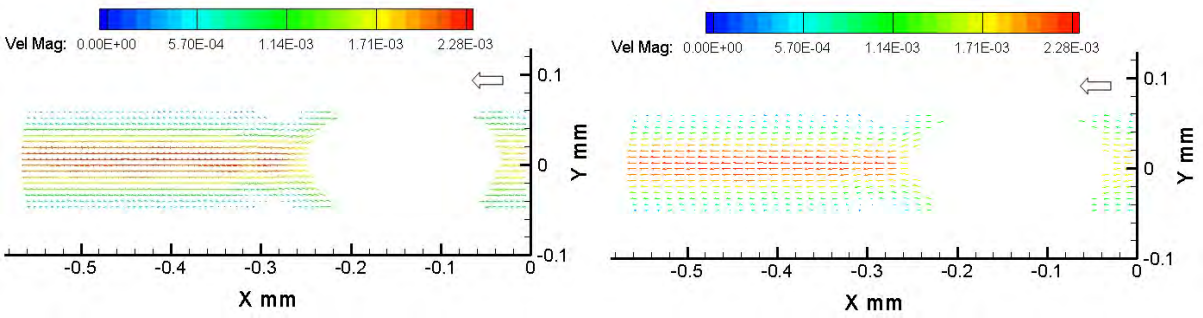

Figure 16. Velocity field of the flow around the first position of the drop in the microchannel with throat

ISSN 2176-5480

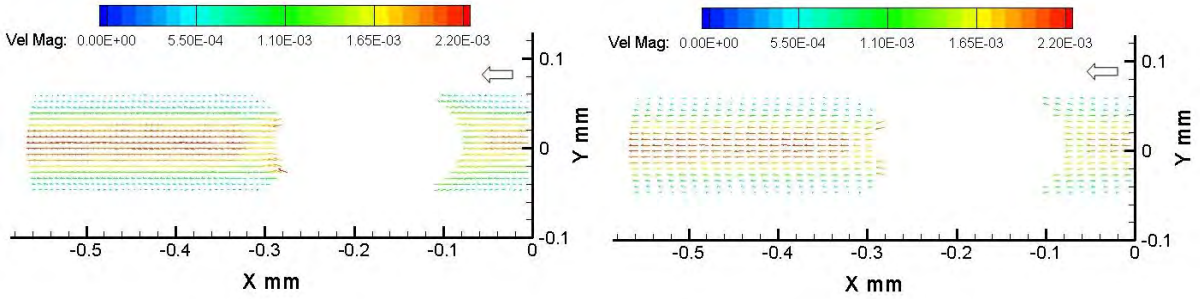

Figure 17. Velocity field of the flow around the second position of the drop in the microchannel with throat

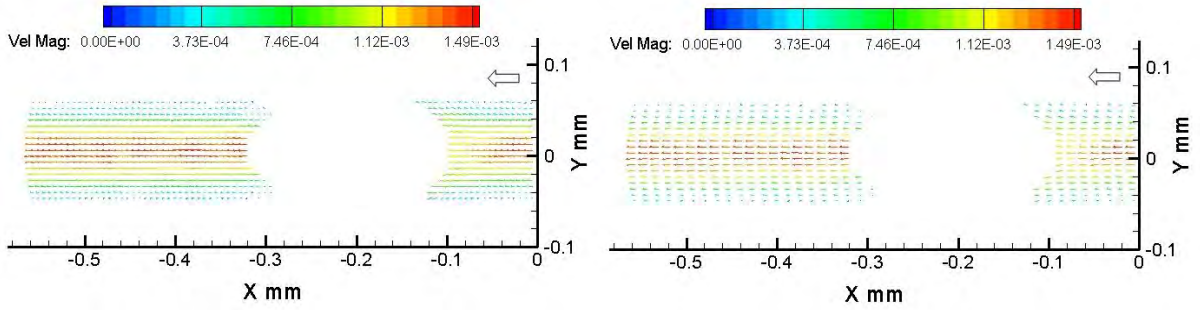

Figure 18. Velocity field of the flow around the third position of the drop in the microchannel with throat

"Figure 19" shows the experimental velocity profiles in the input and output of the flow and the theoretical velocity profile for each position in the throat. "Table 3" shows the velocities obtained for the three positions of the drop. As reference, the average velocity of the injected flow and the average experimental velocities in the input and output of the capillary are also presented.

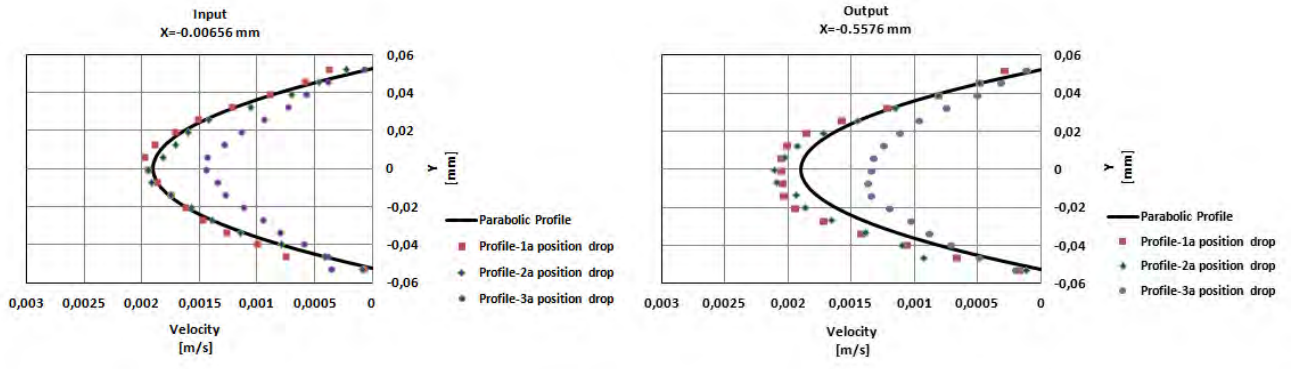

Figure 19. Comparison of parabolic profile and the experimental velocity profiles in the input and output of the flow around the drop through the microchannel with throat, in the three positions.

Table 3. Velocity values of flow and the drop through the microchannel with throat, in the three positions

Drop α=1.4	$V_{average}$ (V_m) Injection flow ($x10^{-4}$ m/s)	$V_{average}$ Exp. Input profile ($x10^{-4}$ m/s)	$V_{average}$ Exp. Output profile ($x10^{-4}$ m/s)	$(V_g)_F$ Front Drop Veloc. ($x10^{-4}$ m/s)	$(V_g)_R$ Rear Drop Veloc. ($x10^{-4}$ m/s)
1ª - Position	9.499	9.890	10.265	17.085	16.093
2ª - Position	9.499	9.795	10.565	17.136	14.579
3ª - Position	9.499	7.255	6.860	14.135	10.930

The results show that although the imposed flow is constant, o flow presents a transient behavior. The drop while is passing by the throat suffers a large deformation. The reduction of the radius of curvature of the interface leads to a considerable increase in the pressure difference to keep the constant flow. Typically water flows are considered

ISSN 2176-5480

incompressible, due to the compressibility factor of the water is extremely low ($\beta \approx 4x10^{-10}$ Pa^{-1}). However, the flow rate studied in this work is very low ($Q \approx 10^{-11}$ m^3/s), so the effects of compressibility of the liquid become important. The flow variation observed is a manifestation of the effect of compressibility of the liquid. In the three positions relative to the throat, the drop velocity was larger than the average flow velocity such as was observed in the flow through the straight capillary. In the first position, the velocities in the front and rear part of the drop are very similar, the effect of the throat in the flow around the drop is still small. In the second position, the front of the drop is accelerated. In the third position, the drop velocity is lower due to the effect of the decrease the flow caused by the partial block of the throat.

4. CONCLUSIONS

The work presented a study of the single phase (water) and two phase (oil drop suspended in water) flow through a straight and with throat microchannel. These geometries may serve as simplified models of the function of two adjacent pores in a porous medium. The measurement of the velocity field of the continuous phase and drop velocity was determined by the technique of particle image velocimetry in micrometer scale (μ-PIV).

In the analysis of the single phase flow through the straight microchannel, the percentage error between the experimental average velocity and the injected average velocity was only 0.44%, demonstrating the precision of the measurements with the μ-PIV system.

To evaluate the effect of the geometry of the capillary in the single phase flow was used a microchannel with throat. The microchannel has a minimum diameter in the throat of 85μm. The experimental maximum velocities were obtained in the area of the throat of microcapillary and the parabolic shape of the experimental velocity profiles was confirmed. The maximum percentage error of the velocity was approximately 4%.

To evaluate the effects due to the presence of oil drops in the flow was generated a drop size α=1.4. The drop size was larger than the diameter of the microchannel and the fluorescent particles were suspended in the continuous phase. The flow with suspended drops is inherently transient; the measurements using the technique of μ-PIV were extremely complex. This problem was resolved using the fact that the flow was periodic and that all the drops were of the same size. The images number used in the analysis was composed of images obtained in different times, but with different drops in the same position in relation to the throat.

In the analysis of the flow of oil drop through a straight microchannel, the velocity values obtained in the oil-water interface were almost constant, in other words, the drop move at same velocity without deforming. The drop moved at a velocity greater than the average flow approximately 1.5 times greater. The experimental average velocities in the input and output of the flow were compared with the injection flow imposed. The percentage error was of 4.41% and 2.41% respectively. The velocity field relative to the drop was obtained subtracting the drop velocity of the velocity field of the two phase flow. In the velocity field was observed a flow in the central part of the microchannel flowing a greater velocity than the drop (in the same direction) and returning contiguous to the wall of the microcapillary flowing a lower velocity that the drop (in the direction opposite). The reason for this was due to the flow presented a train of drops along the microchannel, and the streamlines confirmed the movement of this flow.

In the analysis of the flow of the oil drop through the microchannel with throat, the flow was evaluated at three different instants of time, which correspond to three different positions of the drop along the throat. In the three positions relative to the throat, the drop velocity was always higher than the average velocity of flow, the same way has happened in the two phase flow through the straight microchannel. It was observed that the velocity along the interface was not constant, because the drop was deformed during the passage by the throat, causing acceleration in the drop according was flowing by smaller sections. The average velocity calculated through the experimental velocity profile in three positions of the drop was not equal to the average velocity imposed. Furthermore, the average velocity varied with the time (drop position). A hypothesis for this phenomenon is that the effects of liquid compressibility may be important in very low flow used in this work.

These results can serve as an important base of comparison and validation for numerical solutions in micrometer scale and low values of the number of capillarity and showed the variation of the flow pattern due to the presence of oil drops, and also provided important information as the oil drops change the mobility of the injected fluid when the same flows through pores with throats smaller than the drops size.

5. ACKNOWLEDGEMENTS

The author acknowledges the support from Brazilian Agencies CAPES and FAPERJ by granting a master's scholarship.

6. REFERENCES

Guillen, V.R., Romero, M.I., Carvalho, M.S. and Alvarado, V., 2012. “Capillary-driven mobility control in macro emulsion flow in porous media”. International Journal of multiphase flow, Vol. 43, p. 62-65.

Ho, B.P., and Leal, L.G., 1975. "The creeping motion of liquid drops through a circular tube of comparable diameter". International Journal of Fluids Mechanics, Vol. 71, p. 361-383.

Lac, E., and Sherwood, J.D., 2009. "Motion of a drop along the centreline of a capillary in a pressure-driven flow". International Journal of Fluids Mechanics, Vol. 640, p. 27-54.

Martinez, M.J., and Udell, K.S., 1990. "Axisymmetric creeping motion of drops through circular tubes". International Journal of Fluids Mechanics, Vol. 210, p. 565-591.

Olbricht, W.L., and Leal, L.G., 1983. "The creeping motion of immiscible drops throug a converging/diverging tube". International Journal of Fluids Mechanics, Vol. 134, p. 329-355.

Prasad, A., 2000. "Particle image velocimetry". International Journal Current Science, Vol. 79, p. 51-60.

Raffel, M., Willert, C., and Kompehans, J., 2002. *Particle Image Velocimetry: A practical Guide*. 1st edition.

Wereley, S.T., Santiago, J.G., Meinhart, C.D., Beebe, D.J. and Adrian, R.J., 1998. "A particle image velocimetry system for microfluidics". Springer-Verlag, Vol. 25, p. 316-319.

7. RESPONSIBILITY NOTICE

The author(s) is (are) the only responsible for the printed material included in this paper.